AIAA JOURNAL
Vol. 47, No. 11, November 2009

Numerical Investigation of Constrained Direct Solutions Using Hamilton's Law

Donald L. Kunz*
Air Force Institute of Technology, Wright-Patterson Air Force Base, Ohio 45433-7765

DOI: 10.2514/1.45673

This paper presents numerical results obtained for a dynamic system that is modeled using Hamilton's law of varying action and for which geometric constraints are enforced explicitly. These results are compared with numerical results for the same system that were obtained from ordinary differential equations, differential-algebraic equations, and a formulation based on Hamilton's law in which the constraints were enforced implicitly. This comparison had two objectives: first, to show that numerical results from the formulation based on Hamilton's law and explicit constraints were equal or superior to results from other formulations; second, to verify that explicit constraints must be enforced at the end of the time step. Both objectives were successfully accomplished.

Nomenclature

a	=	parabola constant
E_i	=	total energy at time step t_i
$\mathbf{F}$	=	external forces acting on the particle
f_c	=	constraint force magnitude
G	=	constraint violation
g	=	gravitational constant
g_1	=	displacement constraint
$\mathcal{H}$	=	Hamiltonian
$\mathbf{i}$	=	unit vector in the x direction
$\mathbf{j}$	=	unit vector in the y direction
$\mathbf{k}$	=	unit vector in the z direction
m	=	particle mass
N	=	number of time steps
$\mathbf{P}$	=	particle momentum
p	=	momentum in the x direction
q	=	momentum in the y direction
$\mathcal{T}$	=	kinetic energy
t	=	time
t_1	=	time at the beginning of a time step
t_2	=	time at the end of a time step
u	=	particle velocity in the x direction
$\mathcal{V}$	=	potential energy
v	=	particle velocity in the y direction
w	=	particle velocity in the z direction
x	=	particle lateral coordinate
y	=	particle longitudinal coordinate
z	=	particle vertical coordinate
ΔE	=	change in total energy
Δt	=	time-step duration
$\delta( )$	=	variation of a quantity
λ	=	Lagrange multiplier
τ	=	nondimensional time
$\cdot$	=	time derivative
$\bar{}$	=	value at a time-step midpoint
$\wedge$	=	value at a time-step endpoint

Presented as Paper 2576 at the AIAA/ASME/ASCE/AHS/ASC Structures, Structural Dynamics, and Materials Conference, Palm Springs, CA, 4–7 May 2009; received 26 May 2009; revision received 21 July 2009; accepted for publication 21 July 2009.

*Associate Professor, Department of Aeronautics and Astronautics. Associate Fellow AIAA.

I. Introduction

OVER approximately the past 30 years, dozens of researchers have investigated the advantages of using Hamilton's law (or Hamilton's law of varying action) to obtain direct solutions for the response of dynamic systems. In this context, direct solutions refer to those solutions obtained without first deriving a set of differential equations. Bailey [1–4] was one of the first to promote the use of Hamilton's law as a means for obtaining direct solutions for discrete and continuous systems. The practicality of the method in obtaining solutions to difficult problems was demonstrated by Hodges [5], who used it to obtain direct solutions to a Sturm–Liouville problem with discontinuous coefficients. Other examples of the applications of the method include the work of Borri et al. [6], Borri and Mantegazza [7], Hodges and Bless [8], Kunz [9], and others.

Baruch and Riff [10] solidified the theoretical legitimacy and the proper formulation of direct solutions using Hamilton's law when they showed that there existed several possible correct formulations. They also investigated the various aspects involved in obtaining accurate numerical results [11,12]. In a majority of the aforementioned investigations and applications, however, the equations obtained from Hamilton's law were derived specifically for a single dynamic system. To develop a general-purpose multibody analysis capability that incorporates direct solution methods, one would prefer that the governing equations for the dynamic system under investigation be built up from libraries of equations for various types of bodies and joints.

Although the cited investigations demonstrate the accuracy of direct solution methods, there are few, if any, numerical investigations that address the accuracy of direct solution methods applied to dynamic systems with explicit constraints. However, much of the knowledge that has been accrued from investigations using time finite elements to obtain numerical solutions for ordinary differential equations [13–16] is applicable to direct solutions. The reason is that direct solution methods in mixed form can easily be shown to yield similar equations to those one would obtain by applying the method of time finite elements to ordinary differential equations in first-order form.

The objectives of this paper are to address the accuracy of direct solutions using Hamilton's law and to investigate means for quantifying the accuracy of those solutions. In [9], for example, the accuracy of the direct solutions obtained for the dynamics of a double pendulum was quantified by comparing those solutions with a truth solution and by measuring the change in total energy. The truth solution consisted of the solution of ordinary differential equations, the accuracy of which had been quantified using the method proposed by Junkins and Lee [17]. Measuring the change in total energy is practical and is a good measure of accuracy for conservative systems. However, comparison with a truth solution is generally inconvenient, because it involves setting up and solving two identical problems.

Therefore, this paper will specifically address the use and characteristics of energy change (for conservative dynamic systems) as a measure of accuracy and will also investigate constraint violation (for constrained dynamic systems) as an additional measure of accuracy.

II. Mathematical Model

The mathematical model that will be used for this investigation represents a particle rolling without friction inside an axially symmetric (circular) parabolic bowl (see Fig. 1). An inertial coordinate system is defined such that the z axis is vertical (positive up), and the x and y axes form a horizontal plane that is tangent to the bottom of the bowl. Gravity acts in the negative z direction.

The particle, while rolling in the circular parabolic bowl, has three coordinates that are reduced to two degrees of freedom when the displacement constraint equation (1) is enforced:

$$g_1(x, y, z) = z - a(x^2 + y^2) = 0 \tag{1}$$

The resulting mathematical system can be solved by using either of two methods: nonlinear differential equations or nonlinear algebraic equations.

If the model is represented mathematically by differential equations, there are at least three alternative formulations that may be used. First, the equations may be written as two nonlinear second-order ordinary differential equations. In that case, the constraint equation is enforced implicitly by directly using it to eliminate one of the coordinates (usually z for this example). Second, the equations may be written as four nonlinear first-order ordinary differential equations, in which the constraint equation is again enforced implicitly. If one desires to include the displacement constraint explicitly, there is a third alternative, in which the model may be formulated as a set of differential-algebraic equations (DAEs). In this case, the governing equations are written as six differential equations and either one or two algebraic equations [18]. The reason for the existence of multiple DAE formulations is that the simplest formulation is index 3 and, in general, DAEs with lower index numbers are more amenable to numerical solution. Therefore, index 3 DAEs are often reformulated into index 2 or index 1 form [18].

Governing equations in the form of nonlinear algebraic equations may be obtained through the use of Hamilton's law of varying action. The number of algebraic equations depends on how Hamilton's law is implemented. In this paper, only mixed formulations will be considered, because the equations are simpler and all of the end conditions are natural, or weak. If Eq. (1) is enforced implicitly, the result is four nonlinear algebraic equations that are analogous to the first-order ordinary differential equations discussed previously. When Eq. (1) is enforced explicitly, the mathematical model obtained from Hamilton's law consists of six nonlinear algebraic equations plus one constraint equation. These equations are analogous to the index 3 form of the DAEs. A formulation consisting of six nonlinear algebraic equations plus two constraint equations, which is analogous to the stabilized index 2 form of the DAEs, may also be obtained from Hamilton's law.

This problem was selected because, although it has little practical value in and of itself, the derivations for a number of different formulations are relatively straightforward. The Cartesian system of coordinates is used because changes to the shape of the bowl (e.g., from circular to elliptical) could be readily accomplished in any of the formulations by an appropriate modification of the constraint equation. Furthermore, the dynamics of the problem are not trivial, and the results should adequately achieve the objectives of this investigation.

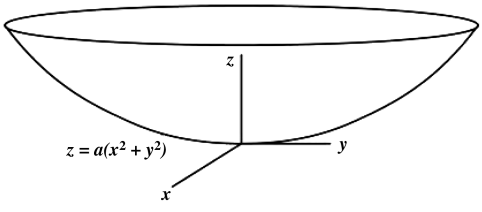

Fig. 1 Axially symmetric parabolic bowl.

A. Derivation of the Ordinary Differential Equations

The ordinary differential equations of motion for the particle can easily be derived using either Newton's second law or Lagrange's equation. Newton's method starts with the calculation of the particle momentum:

$$\mathbf{P} = m\left(\frac{\mathrm{d}x}{\mathrm{d}t}\mathbf{i} + \frac{\mathrm{d}y}{\mathrm{d}t}\mathbf{j} + \frac{\mathrm{d}z}{\mathrm{d}t}\mathbf{k}\right) \tag{2}$$

The external forces acting on the particle include the gravitational force, which acts in the z direction, and the constraint force, which acts in a direction normal to the surface of the bowl:

$$\mathbf{F} = f_c\frac{\nabla g_1}{|\nabla g_1|} - mg\mathbf{k} \tag{3}$$

Newton's second law sets the time derivative of Eq. (2) equal to Eq. (3), which yields one equation in each of the **i**, **j**, and **k** directions. After solving the **k** equation for f_c, and substituting the result for f_c into the **i** and **j** equations, two second-order differential equations are obtained. These can be transformed into first-order form, yielding Eqs. (4–7):

$$\frac{\mathrm{d}x}{\mathrm{d}t} = u \tag{4}$$

$$\frac{\mathrm{d}y}{\mathrm{d}t} = v \tag{5}$$

$$(1 + 4a^2x^2)\frac{\mathrm{d}u}{\mathrm{d}t} + 4a^2xy\frac{\mathrm{d}v}{\mathrm{d}t} = -[4a^2x(u^2 + v^2) + 2gax] \tag{6}$$

$$4a^2xy\frac{\mathrm{d}u}{\mathrm{d}t} + (1 + 4a^2y^2)\frac{\mathrm{d}v}{\mathrm{d}t} = -[4a^2y(u^2 + v^2) + 2gay] \tag{7}$$

In addition to the differential equations of motion, an equation can be written for the magnitude of the constraint force, as a function of the particle position and velocity:

$$f_c = m\frac{g + 2a(u^2 + v^2)}{\sqrt{1 + 4a^2(x^2 + y^2)}} \tag{8}$$

Lagrange's equation can also be used to derive the ordinary differential equations for the particle. The kinetic and potential energies of the particle are defined in Eqs. (9) and (10), respectively:

$$\mathcal{T} = \frac{1}{2}m\left[\left(\frac{\mathrm{d}x}{\mathrm{d}t}\right)^2 + \left(\frac{\mathrm{d}y}{\mathrm{d}t}\right)^2 + \left(\frac{\mathrm{d}z}{\mathrm{d}t}\right)^2\right] \tag{9}$$

$$\mathcal{V} = -mgz \tag{10}$$

After using Eq. (1) and its time derivative to substitute for z and its derivative in Eqs. (9) and (10), Lagrange's equation yields two second-order ordinary differential equations. When transformed to first-order form, Eqs. (4–7) are obtained. However, Lagrange's equation does not yield an expression for the constraint force.

B. Derivation of the Differential-Algebraic Equations

The differential-algebraic equations for the particle are also obtained from the kinetic and potential energies in Eqs. (9) and (10). In this derivation, however, Eq. (1) is not substituted directly to eliminate the dependent coordinate. Instead, it serves as an independent constraint equation that is coupled to the differential equations using a Lagrange multiplier [19]. The resulting equations of motion are shown as Eqs. (11–17), where λ is the Lagrange multiplier:

$$\frac{\mathrm{d}x}{\mathrm{d}t} = u \tag{11}$$

$$\frac{\mathrm{d}y}{\mathrm{d}t} = v \tag{12}$$

$$\frac{\mathrm{d}z}{\mathrm{d}t} = w \tag{13}$$

$$\frac{\mathrm{d}u}{\mathrm{d}t} = -\frac{2ax}{m}\lambda \tag{14}$$

$$\frac{\mathrm{d}v}{\mathrm{d}t} = -\frac{2ay}{m}\lambda \tag{15}$$

$$\frac{\mathrm{d}w}{\mathrm{d}t} = -g + \frac{1}{m}\lambda \tag{16}$$

$$z - a(x^2 + y^2) = 0 \tag{17}$$

Note that Eqs. (11), (12), and (17) are identical to Eqs. (4), (5), and (1), respectively. It is also pertinent to note that Eqs. (11–17) form a set of semi-implicit index 3 DAEs.

The index number of the DAEs can be reduced to semi-implicit index 2 form by replacing Eq. (17) with its derivative, Eq. (18):

$$w - 2a(xu + yw) = 0 \tag{18}$$

Although this procedure does reduce the index number, it has been observed [18] that numerical solutions tend to drift because the displacement constraint is not being enforced explicitly. The index may be further reduced by replacing Eq. (18) with its derivative, the result being a set of DAEs in semi-implicit index 1 form.

C. Derivation of the Algebraic Equations from Hamilton's law

Starting with the kinetic and potential energies from Eqs. (9) and (10), we again substitute for z and its time derivative based on Eq. (1). Hamilton's law of varying action may then be expressed as shown in Eq. (19):

$$\delta \int_{t_1}^{t_2} (\mathcal{T} - \mathcal{V})\,\mathrm{d}t - \delta x p|_{t_1}^{t_2} - \delta y q|_{t_1}^{t_2} = 0 \tag{19}$$

The end terms in Eq. (19) are expressed in terms of the momenta p and q, and the kinetic energy may be expressed in terms of these quantities as well. The momenta, rather than velocities, are used in this case simply to make the algebraic manipulations that follow easier to manage. To take full advantage of Hamilton's law, Eq. (19) should also be expanded and cast in its weakest possible form, which results in a mixed formulation in which all of the end conditions are natural:

$$\int_{t_1}^{t_2} (\delta\dot{x}p - \delta\dot{p}x + \delta\dot{y}q - \delta\dot{q}y - \delta\mathcal{H})\,\mathrm{d}t + \delta p x|_{t_1}^{t_2} - \delta x p|_{t_1}^{t_2} + \delta q y|_{t_1}^{t_2} - \delta y q|_{t_1}^{t_2} = 0 \tag{20}$$

The Hamiltonian $\mathcal{H}$ is expressed as follows:

$$\mathcal{H} = \frac{1}{2}\frac{(1 + 4a^2y^2)p^2 + (1 + 4a^2x^2)q^2 - 8a^2xypq}{m(1 + 4a^2x^2 + 4a^2y^2)} + mga(x^2 + y^2) \tag{21}$$

Equation (20), which is often called Hamilton's weak principle, can now be expanded with the goal of collecting the coefficients of the variations of the generalized coordinates. To achieve that goal, two more steps are needed. First, time is nondimensionalized according to Eq. (22):

$$\tau = \frac{t - t_1}{t_2 - t_1} = \frac{t - t_1}{\Delta t} \tag{22}$$

Then both the generalized coordinates and their variations are discretized. Equation (20) was purposely derived in a manner such that no time derivatives of the generalized coordinates appear in the equation. This means that the shape functions that are used to discretize the generalized coordinates may be constant over each time step. On the other hand, time derivatives of the variations of the generalized coordinates do appear, and so their shape functions must be linear. Equations (23) and (24) serve as examples of how the discretization was performed for all of the generalized coordinates and their variations:

$$x = \begin{cases} \hat{x}_1 & \tau = 0 \\ \bar{x} & 0 < \tau < 1 \\ \hat{x}_2 & \tau = 1 \end{cases} \tag{23}$$

$$\delta x = \delta x_1(1 - \tau) + \delta x_2 \tau \tag{24}$$

Clearly, the hatted quantities in Eqs. (23) and (24) represent the values of the generalized coordinates at the ends of the time step, and the barred quantities represent the values of the generalized coordinates at the midpoint of the time step.

Once the substitutions of the discretizations for the generalized coordinates and their variations have been performed, the coefficients of the variational quantities (e.g., δx_1) can be identified and set equal to zero. These eight nonlinear algebraic equations can be solved directly for the dynamic response. However, it can be observed that when the pairs of equations associated with each generalized coordinate are subtracted from one another, one obtains the result that the barred quantities are the averages of the hatted quantities. For example,

$$\bar{x} = \frac{\hat{x}_1 + \hat{x}_2}{2} \tag{25}$$

Then, the pairs of equations can be added to one another, the barred quantities can be eliminated, and only four equations need to be solved simultaneously. Equations (26–29) are the resulting nonlinear algebraic equations:

$$\hat{p}_2 - \hat{p}_1 + \Delta t\left\{2mga\bar{x} + \frac{4a^2(\bar{x}\,\bar{q} - \bar{y}\,\bar{p})\bar{q}}{m(1 + 4a^2\bar{x}^2 + 4a^2\bar{y}^2)} - \frac{4a^2\bar{x}[(1 + 4a^2\bar{y}^2)\bar{p}^2 + (1 + 4a^2\bar{x}^2)\bar{q}^2 - 8a^2\bar{x}\,\bar{y}\,\bar{p}\,\bar{q}]}{m(1 + 4a^2\bar{x}^2 + 4a^2\bar{y}^2)^2}\right\} = 0 \tag{26}$$

$$\hat{q}_2 - \hat{q}_1 + \Delta t\left\{2mga\bar{y} + \frac{4a^2(\bar{y}\,\bar{p} - \bar{x}\,\bar{q})\bar{p}}{m(1 + 4a^2\bar{x}^2 + 4a^2\bar{y}^2)} - \frac{4a^2\bar{y}[(1 + 4a^2\bar{y}^2)\bar{p}^2 + (1 + 4a^2\bar{x}^2)\bar{q}^2 - 8a^2\bar{x}\,\bar{y}\,\bar{p}\,\bar{q}]}{m(1 + 4a^2\bar{x}^2 + 4a^2\bar{y}^2)^2}\right\} = 0 \tag{27}$$

$$\hat{x}_2 - \hat{x}_1 - \Delta t\left[\frac{(1 + 4a^2\bar{y}^2)\bar{p} - 4a^2\bar{x}\,\bar{y}\,\bar{q}}{m(1 + 4a^2\bar{x}^2 + 4a^2\bar{y}^2)}\right] = 0 \tag{28}$$

$$\hat{y}_2 - \hat{y}_1 - \Delta t\left[\frac{(1 + 4a^2\bar{x}^2)\bar{q} - 4a^2\bar{x}\,\bar{y}\,\bar{p}}{m(1 + 4a^2\bar{x}^2 + 4a^2\bar{y}^2)}\right] = 0 \tag{29}$$

D. Algebraic Equations from Hamilton's Law with Appended Constraints

The derivation of the nonlinear algebraic equations used to obtain direct solutions from Hamilton's law when constraints are appended

proceeds in a manner that is very similar to the derivation in the previous subsection. Therefore, steps that are identical in both derivations will not be described again. One significant difference is the starting point for the derivation. Because of the displacement constraint, Eq. (19) must be modified by appending the constraint equation with a Lagrange multiplier as follows:

$$\delta \int_{t_1}^{t_2} [\mathcal{T} - \mathcal{V} + \lambda g_1(x, y, z)]\, \mathrm{d}t - \delta x p|_{t_1}^{t_2} - \delta y q|_{t_1}^{t_2} = 0 \tag{30}$$

where g_1 is the displacement constraint:

$$g_1 = z - a(x^2 + y^2) \tag{31}$$

For this formulation of the problem, it turns out that using the momenta is more complicated algebraically than using the velocities. Therefore, Hamilton's weak principle for this formulation takes the form of Eq. (32):

$$\begin{aligned}\int_{t_1}^{t_2} \{&\delta \dot{x} m u - \delta \dot{u} m x + \delta \dot{y} m v - \delta \dot{v} m y + \delta \dot{z} m w - \delta \dot{w} m z - m(\delta u u \\ &+ \delta v v + \delta w w) - \delta z m g + \delta \lambda [z - a(x^2 + y^2)] + [\delta z \\ &- 2a(\delta x x + \delta y y)]\lambda\}\, \mathrm{d}t + \delta u m x|_{t_1}^{t_2} + \delta v m y|_{t_1}^{t_2} + \delta w m z|_{t_1}^{t_2} \\ &- \delta x m u|_{t_1}^{t_2} - \delta x m v|_{t_1}^{t_2} - \delta z m w|_{t_1}^{t_2} = 0\end{aligned} \tag{32}$$

From this point forward, the procedure for deriving the nonlinear algebraic equations follows the procedure used in the last subsection. That is, time is nondimensionalized according to Eq. (22), and the generalized coordinates are discretized in a manner identical to Eqs. (23) and (24). One difference is that there are no time derivatives of $\delta\lambda$ and so it may be discretized according to Eq. (23). Once again, after the discretization substitutions are made, the coefficients of the variational quantities are collected and set equal to zero. By summing and differencing the pairs of equations associated with each generalized coordinate, six equations in the form of Eq. (25) are obtained, as are seven equations that can be solved to obtain the dynamic response of the system:

$$m(\hat{x}_2 - \hat{x}_1) - m\bar{u}\Delta t = 0 \tag{33}$$

$$m(\hat{y}_2 - \hat{y}_1) - m\bar{v}\Delta t = 0 \tag{34}$$

$$m(\hat{z}_2 - \hat{z}_1) - m\bar{w}\Delta t = 0 \tag{35}$$

$$m(\hat{u}_2 - \hat{u}_1) + 2a\bar{x}\,\bar{\lambda}\,\Delta t = 0 \tag{36}$$

$$m(\hat{v}_2 - \hat{v}_1) + 2a\bar{y}\,\bar{\lambda}\,\Delta t = 0 \tag{37}$$

$$m(\hat{w}_2 - \hat{w}_1) + (mg - \bar{\lambda})\Delta t = 0 \tag{38}$$

$$\bar{z} - a(\bar{x}^2 + \bar{y}^2) = 0 \tag{39}$$

Note that Eqs. (33–39) are very similar in form to Eqs. (11–17). This suggests that the equations derived from Hamilton's law are simply a different form of the semi-implicit index 3 DAEs. It is also important to note that the generalized coordinates in Eq. (39) are barred, indicating that they are values at the midpoint of the time step. Because this equation is equivalent to the constraint equation (31), the derivation suggests that the displacement constraint should be enforced at the midpoint of the time step. Further discussion of this issue will be addressed in the following section.

III. Numerical Results

The numerical results to follow were calculated using Octave, an open-source clone of MATLAB. In this investigation, the LSODE (Adams predictor–corrector) algorithm [20,21] that is implemented in Octave has been used (with all of the default options) to solve the ordinary differential equations derived in Sec. II.A. The nonlinear algebraic equations derived in Secs. II.C and II.D have been solved using Powell's hybrid method [22]. This algorithm has been implemented as the Fortran subroutine HYBRD and is also included in Octave. All of the default options in the Octave implementation of HYBRD have been used. A limited number of numerical solutions of the DAEs derived in Sec. II.B were obtained using the Octave implementation of DASPK, an updated implementation of DASSL [18].

All of the numerical results presented in this paper have been calculated with values of $m = 1.0$ kg, $a = 0.5$ 1/m, and $g = -9.806555$ m/s. The initial conditions for the particle are $x(0) = 1.0$ m, $y(0) = 0.0$ m, $u(0) = 0.0$ m/s, and $v(0) = 0.2$ m/s. Initial values for z and w, when needed, were calculated from Eqs. (1) and (18). For a simulation to start correctly for a general set of initial conditions, those initial conditions must also satisfy Eqs. (1) and (18). The simulations in this paper were all run for 5.0 s using various time-step sizes. Figure 2 shows the displacements and velocities of the particle calculated from the ordinary differential equations using a time step of 0.05 s. Because all other successfully calculated solutions are sufficiently accurate that their differences cannot be observed in displacement and velocity plots, Fig. 2 will serve as being typical of all such solutions.

For all of the cases to follow, the change in total energy from the value at the initial state of the system will be displayed. Herein, total energy is defined as the sum of the kinetic energy equation (9) and potential energy equation (10). The norm and the rms values of the change in total energy over the duration of the simulation will be calculated according to Eqs. (40) and (41). Percent energy change may be obtained by multiplying by 100:

$$\|\Delta E\| = \sqrt{\sum_{i=0}^{N} \Delta E_i^2}; \qquad \Delta E_i \equiv \frac{E(t = t_i) - E(t = t_0)}{E(t = t_0)} \tag{40}$$

$$\Delta E_{\mathrm{rms}} = \sqrt{\frac{1}{N}\|\Delta E\|} \tag{41}$$

For the cases in which the constraint equations are explicit, the norm and rms values of the constraint violation G over the duration of the simulation will be calculated according to algorithms similar to that used for the energy change:

$$\|G\| = \sqrt{\sum_{i=0}^{N} g_1^2(t = t_i)} \tag{42}$$

$$G_{\mathrm{rms}} = \sqrt{\frac{1}{N}\|G\|} \tag{43}$$

Because Eqs. (42) and (43) define the norm and rms displacement constraint violation over the time interval, the definitions for the norm and rms velocity constraint violation are obtained by substituting the left-hand side of Eq. (18) for g_1 in Eqs. (42) and (43).

A. Ordinary Differential Equations

As explained previously, the ordinary differential equations for the motion of a particle in a circular parabolic bowl were solved using the LSODE algorithm. Because [9] demonstrated that this algorithm displays sufficient accuracy using inverse dynamics [17], no additional validation will be presented. However, for the purposes of comparing these results with direct solutions, we need to look at energy conservation. The solution from LSODE returns x, y, u, and v at the end of each time step, from which z and w, followed by the total energy, may be calculated.

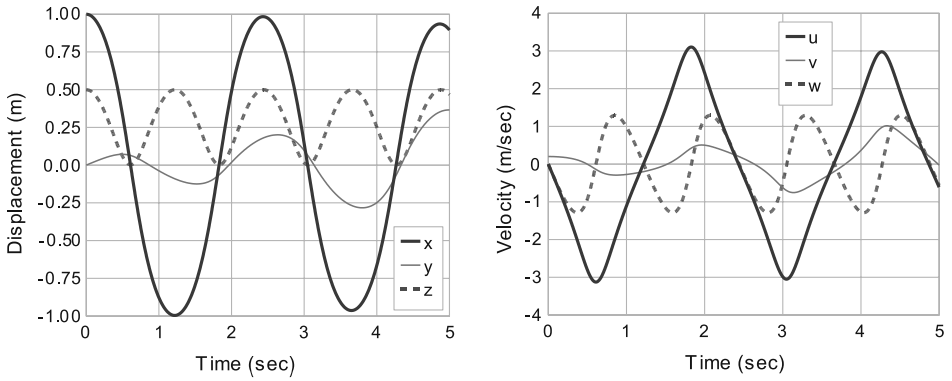

a) Displacement **b) Velocity**

Fig. 2 Particle displacement and velocity vs time.

Figure 3a shows the norm and rms values of the change in energy as the size of the time step is varied. Curiously, the norm of the energy change increases as the size of the time step decreases, whereas the rms value of the energy change remains relatively constant. The reason for this behavior is that whereas the energy change per time step does decrease as the time step decreases in size, the number of time steps for the 5.0 s simulation increases at a rate that makes the solution appear to get less accurate as the sizes of the time steps decrease. The rms value of the energy change actually gives a more accurate estimate of the error.

When the energy change ΔE_i is viewed as a function of time for each time-step size, one can see that the change in energy is nearly identical for all time-step sizes. Figure 3b, which is typical of all of the other energy-change-vs-time plots, shows that there is a small net loss of energy over the duration of the simulation. The loss of energy averages between 0.20×10^{-6} and 0.24×10^{-6} per second. This rate of energy loss should not cause significant problems unless the simulation approaches 10,000 s in duration.

B. Differential-Algebraic Equations

The algorithm DASPK used in this investigation to obtain numerical solutions for DAEs was designed to solve only index 1 DAEs. Indeed, experimentation showed that numerical solutions for the semi-explicit index 3 form shown in Eqs. (11–17) could not be obtained from DASPK. However, numerical solutions for the semi-explicit index 2 form [Eqs. (11–16) and (18)] could be obtained when the algebraic variables were excluded from the error estimate. Presumably, the reason that it was possible to obtain these solutions was that as a rule, a semi-implicit case behaves much like the general case of one index lower. Because DASPK was designed to solve index 1 DAEs, solutions for semi-implicit index 2 DAEs may also be obtained. For this formulation, DASPK returns x, y, z, u, v, w, and λ at each time step, from which the total energy and constraint violation may be calculated.

Results for the change in energy during a 5 s simulation are shown in Fig. 4. Figure 4a indicates that the rms value of the energy change is invariant with time step. However, a comparison of Fig. 4a with Fig. 3a shows that the rms energy change for the DAE solution is several orders of magnitude larger than the rms energy change for the ordinary differential equation (ODE) solution. The energy change as a function of time for a step size of 0.001 s is shown in Fig. 3b. It is interesting to note that the shape of the curve in Fig. 3b is virtually identical for all time-step sizes.

The accuracy of the solution of the semi-implicit index 2 DAEs as measured by the violation of the velocity and displacement constraints is shown in Figs. 5 and 6. The result of the index reduction from index 3 to index 2 was that the velocity constraint was being enforced by the DAEs, whereas the displacement constraint was not being enforced. In Fig. 5a, it can be seen that the rms value of the velocity constraint violation is acceptably small and relatively constant with the size of the time step. Figure 5b shows that, apart from small intermittent deviations, the velocity constraint is being well enforced.

Figure 6 illustrates the behavior of the displacement constraint, which is not being explicitly enforced in the DAEs. As seen in Fig. 6a, the rms value of the constraint violation is only an order of magnitude larger than the rms value of the velocity constraint violation. Furthermore, as in the case of the velocity constraint, the displacement constraint violation is relatively insensitive to the time-step size. However, the problem of drift, discussed in Sec. II.B, is evident in Fig. 6b. The constraint violation at any selected time is small, but is not as well-behaved as the velocity constraint in Fig. 5b.

C. Implicit Direct Solution

The implicit formulation of the direct solution, as derived in Sec. II.C, was obtained by substituting the displacement and velocity constraint equations directly into the kinetic and potential energy. The four resulting nonlinear algebraic equations (26–29) can be

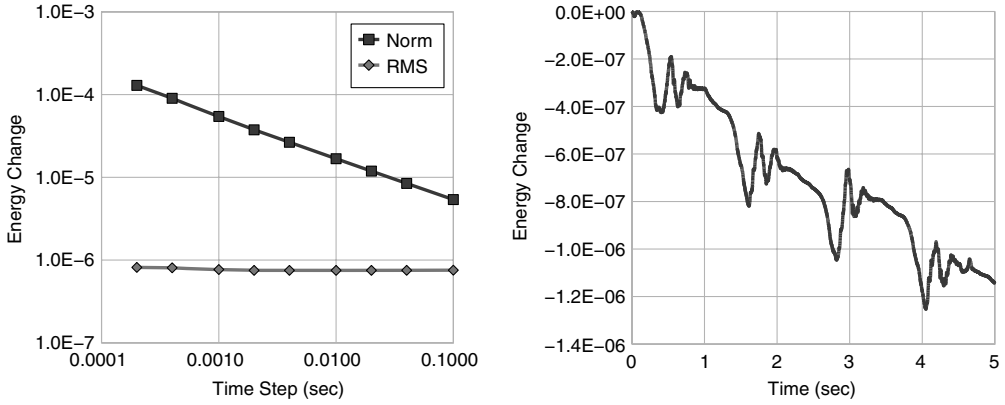

a) Norm and rms values of energy change **b) Energy change for $\Delta t = 0.001$ s**

Fig. 3 Solutions from the ordinary differential equations.

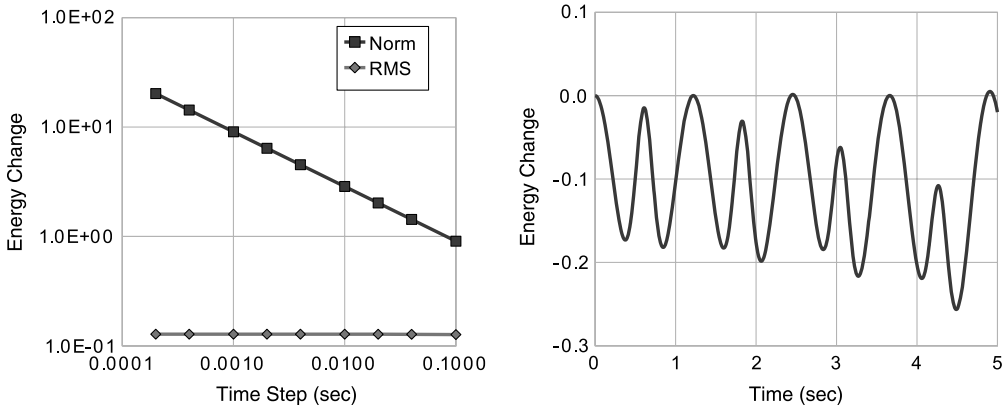

a) Norm and rms values of energy change **b) Energy change for $\Delta t = 0.001$ s**

Fig. 4 Solutions from the semi-implicit index 2 differential-algebraic equations.

solved using the HYBRD algorithm. A comparison of these equations with the ordinary differential equations (4–7) reveals strong similarities. The solution of the nonlinear algebraic equations at each time step returns x, y, p, and q, from which u and v may be computed, followed by the calculation of the total energy.

The norm and rms values for a range of time-step sizes are displayed in Fig. 7a. The trends in those curves are much different from the curves in Fig. 3a, because the norm and rms values in Fig. 7a both decrease with decreasing step size. However, there is a difference in slope, which again results from the fact that the calculation of the norm does not account for the increase in the number of time steps as the step size decreases. It also appears that there is a break-even point at a step size of approximately 0.002 s. Above that value, the ODE solution is superior, whereas at smaller step sizes, the implicit direct solution is better. Figure 7a shows that the point at which round-off error begins to overshadow the truncation (time-step size) error was not reached. However, at a time-step size of 0.0004 s, high-frequency oscillations in the energy began to appear and grew larger at the 0.0002 s time-step size. Therefore, further reductions in the size of the time step were halted.

It is apparent by comparing Fig. 7b with Fig. 3b that the characteristics of the change in total energy for the two solution methods are very different. The energy change for the direct solution is periodic, with a period approximately equal to the period of the z

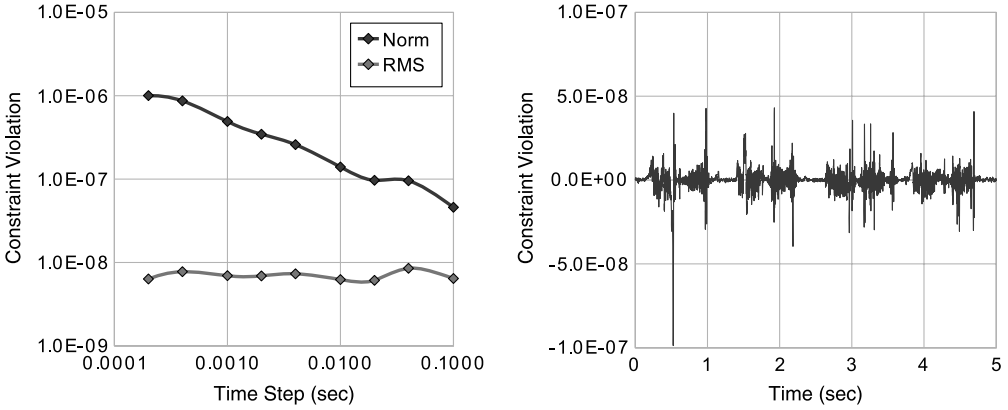

a) RMS values for a range of time step sizes **b) Velocity constraint violation for $\Delta t = 0.001$ s**

Fig. 5 Velocity constraint violation for semi-implicit index 2 differential-algebraic equations.

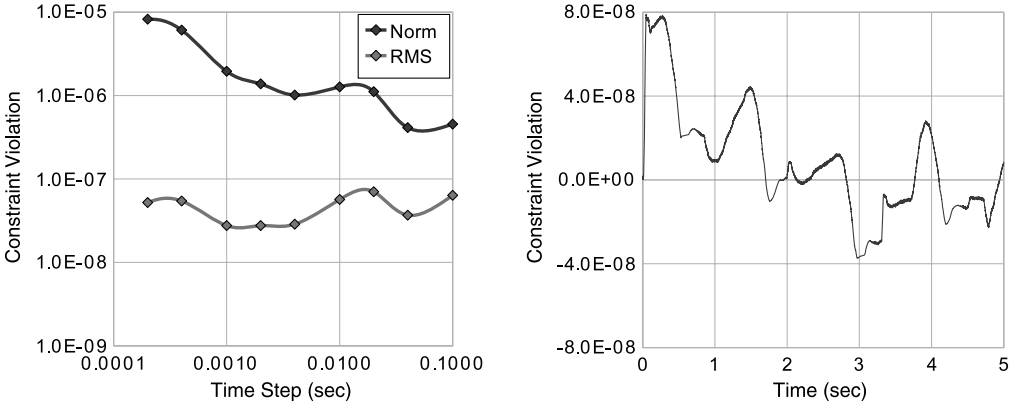

a) Norm and rms values for a range of time step sizes **b) Displacement constraint violation for $\Delta t = 0.001$ s**

Fig. 6 Displacement constraint violation for semi-implicit index 2 differential-algebraic equations.

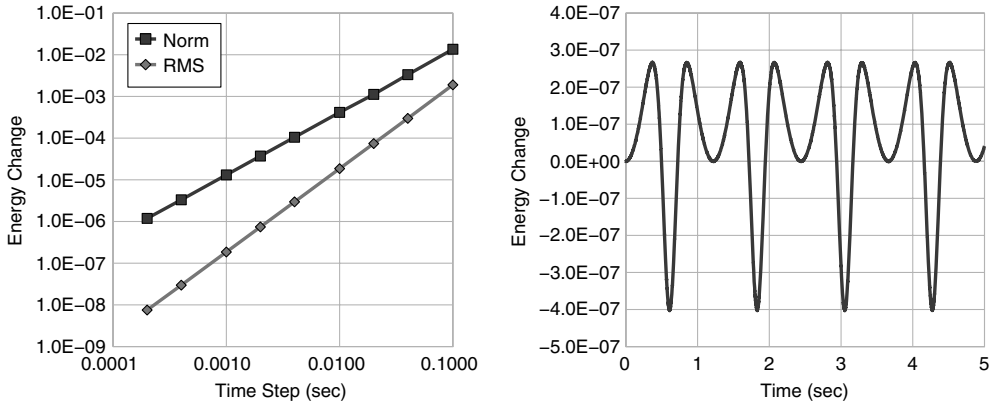

a) Norm and rms values of energy change **b) Energy change for $\Delta t = 0.001$ s**

Fig. 7 Direct solutions from Hamilton's law with implicit constraints.

displacements; and the greatest difference in energy occurs when the particle reaches its lowest point in the bowl. Longer simulations have demonstrated that for a specified time step, the periodicity of the direct solution is maintained, whereas the ODE solution continues to lose energy. Therefore, when energy conservation is used as a measure of solution accuracy, the direct method outperforms the ODE solution method, even for simulations of relatively short duration. Also, whereas step size has a relatively insignificant effect on the energy loss in the ODE solution, the amplitude of the periodic variations in energy from the direct solution can be reduced by decreasing the time step.

D. Explicit Direct Solution with Displacement Constraints

In the previous subsection, it was demonstrated that a direct solution of nonlinear algebraic equations with implicit constraints, which correspond closely to the first-order differential equations for the same system, may be at least as accurate, if not more so, as the solution obtained from differential equations. Now we wish to compare direct solutions for a set of equations in which the constraints are explicit to direct solutions from the equations with implicit constraints. For this formulation, the numerical algorithm returns x, y, z, u, v, w, and λ at each time step, from which the total energy and constraint violation may be calculated.

In this subsection, the displacement constraints will be enforced in a manner analogous to the semi-implicit index 3 form of the DAEs in Sec. II.B. Two cases will be considered. The first case is one in which the displacement constraint is enforced at the midpoint of the time step, as suggested by Eq. (39). In the second case, the displacement constraint is enforced at the end of the time step, as suggested by [23]. Powell's hybrid method is used to solve the equations for the first case, which include Eqs. (33–39). The same algorithm is used to solve the same set of equations for the second case, with the exception that $\bar{x} = \hat{x}$, $\bar{y} = \hat{y}$, and $\bar{z} = \hat{z}$ in Eq. (39).

As discussed in Sec. II.D, a strict development of the equations results in the constraints being enforced at the midpoint of the time step. The plots in Fig. 8 show the change in energy that results from enforcing the displacement constraint in this manner. Both the norm and rms values of the energy change are unacceptably large for all time-step sizes, and as shown in Fig. 8b, these values result from a dramatic increase in energy that starts approximately 3.5 s into the simulation.

According to Fig. 9a, the displacement constraint is working as one would expect. That is, the displacement constraint violation at the midpoint is small, because that constraint is being enforced, and the constraint violation at the endpoint, although orders of magnitude larger, is satisfactory and decreases as the size of the time step decreases. Figure 9b, however, shows a disturbing trend in which the constraint violation oscillates at a high frequency and (relatively) large amplitude as the simulation nears its end. This disturbing trend is reinforced by the velocity constraint violation shown in Fig. 10. Although the rms value of the velocity constraint violation at the midpoint decreases with decreasing time-step sizes, as it should, Fig. 10a shows the constraint violation at the endpoint to be unacceptably large and mostly unaffected by decreasing the time-step size. This observation is borne out by extremely large oscillations in the violation of the endpoint velocity constraint, as shown in Fig. 10b, and also provides the explanation for the large excursions in energy change shown in Fig. 8b. It would appear that the displacements and velocities are allowed to drift from the midpoint to the endpoint of each time step. In subsequent steps, the midpoint constraint is enforced, but the starting value is compromised due to the inaccuracy of the endpoint from the previous step [see Eq. (25)] and yields a less accurate result at the end of the current step. As the simulation proceeds, these errors cascade until the solution algorithm is overwhelmed and fails.

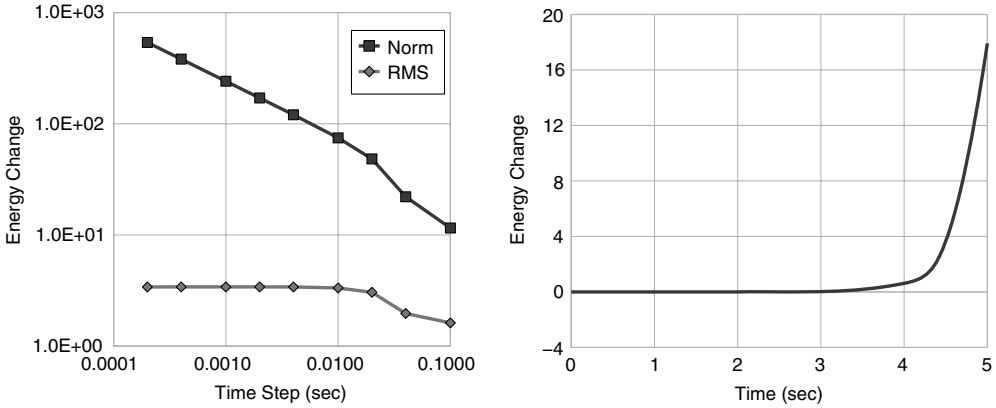

a) Norm and rms values of energy change **b) Energy change for $\Delta t = 0.001$ s**

Fig. 8 Direct solutions from Hamilton's law with explicit midpoint displacement constraints.

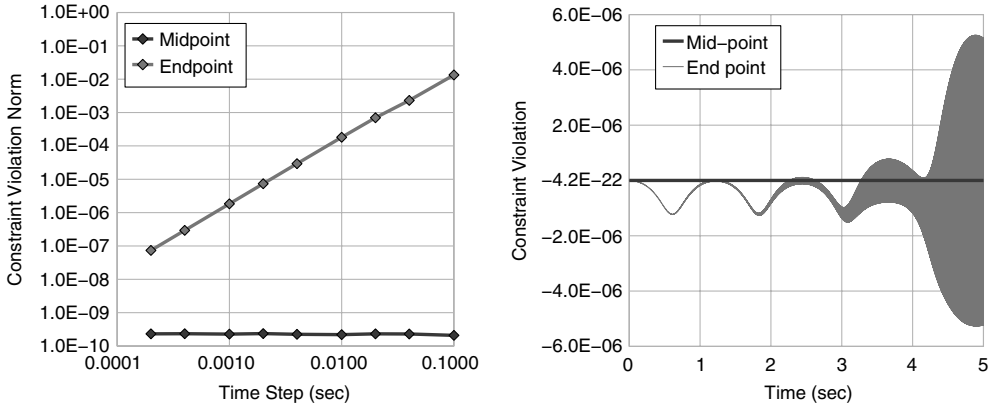

a) RMS values for a range of time step sizes **b) Displacement constraint violation for Δt =0.001 s**

Fig. 9 Displacement constraint violation for explicit displacement constraints enforced at the midpoint.

The second case, in which the displacement constraint is enforced at the endpoints of the time steps, shows very different behavior as compared with the first case. The rms values of the energy change, as shown in Fig. 11a, are very small (less than 10^{-9}) when the displacement constraint is enforced at the endpoints of the time steps, and they are relatively unaffected by the size of the time step. The increase in the norm of the energy change with decreasing time-step size is again merely an artifact of the number of steps not being taken into account. Figure 11b shows that the energy change is prone to oscillate, but the amplitudes are insignificant for sufficiently small time steps. A comparison of the magnitudes of the energy oscillations in Figs. 7 and 11 indicates that direct solutions with explicit constraints enforced at the endpoints actually outperform direct solutions with implicit constraints.

Because the displacement constraints are being enforced at the endpoints, the amount of displacement constraint violation at the endpoints, as shown in Fig. 12, is extremely small (on the order of machine precision) and unaffected by time-step size. As one would expect, Fig. 13a shows that decreasing the size of the time step also decreases the norm and rms values of the velocity constraint violation. With a sufficiently small time step, the constraint violation can be reduced to acceptable levels. As illustrated in Fig. 13b, the change in velocity constraint violation is periodic, with a period approximately equal to the period of the z coordinate.

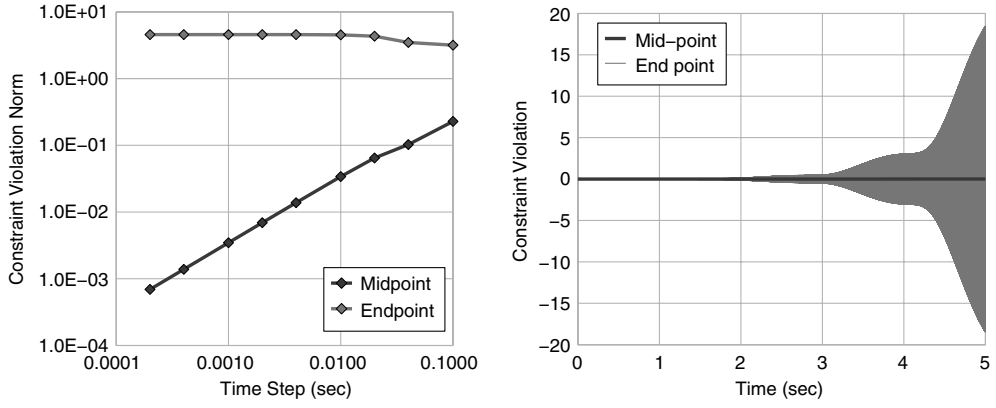

a) RMS values for a range of time step sizes **b) Velocity constraint violation for Δt = 0.001 s**

Fig. 10 Velocity constraint violation for explicit displacement constraints enforced at the midpoint.

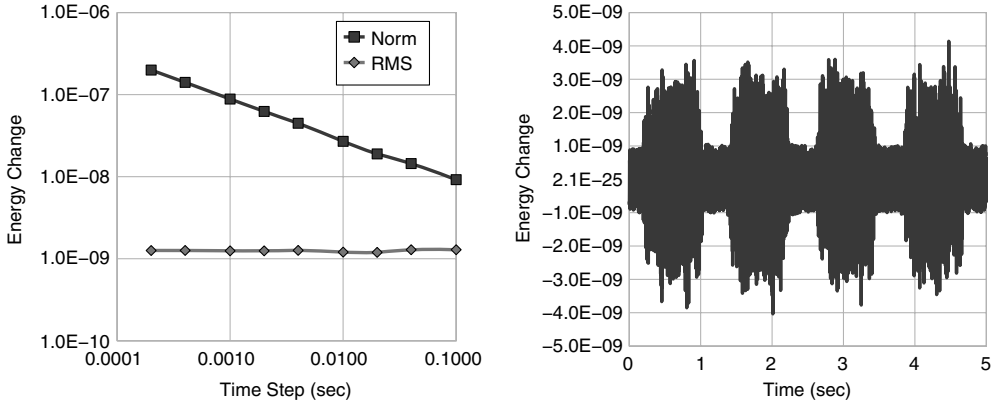

a) Norm and rms values of energy change **b) Energy change for Δt = 0.001 s**

Fig. 11 Direct solutions from Hamilton's law with explicit endpoint displacement constraints.

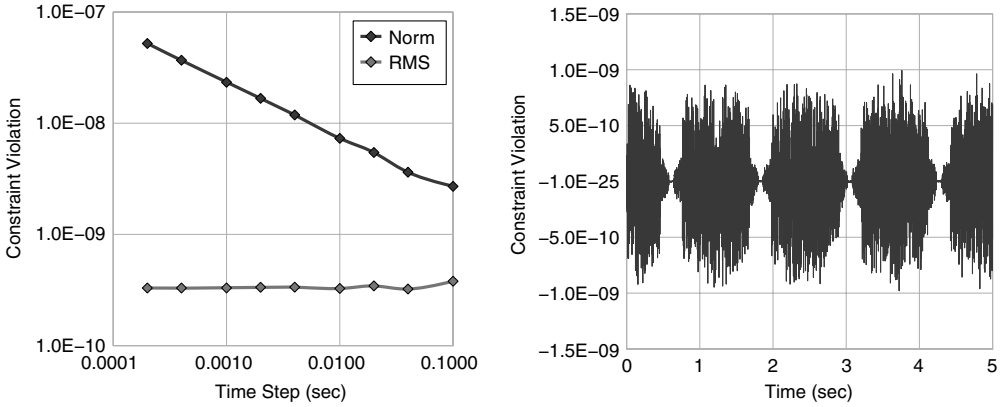

a) Norm and rms values for a range of time step sizes **b) Displacement constraint violation for $\Delta t = 0.001$ s**

Fig. 12 Displacement constraint violation for explicit displacement constraints enforced at the endpoint.

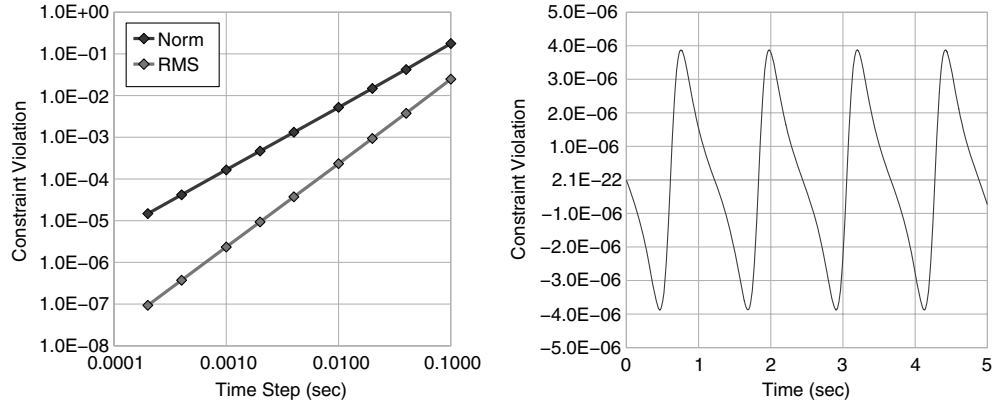

a) RMS values for a range of time step sizes **b) Velocity constraint violation for $\Delta t = 0.001$ s**

Fig. 13 Velocity constraint violation for explicit displacement constraints enforced at the endpoint.

IV. Conclusions

This paper has compared the accuracy of results from simulations of a dynamic system using a variety of numerical solution methods. These solution methods included time integration of ordinary differential equations and differential-algebraic equations, direct solutions of nonlinear algebraic equations derived from Hamilton's law in which the constraints were implicit, and similar direct solutions of equations in which the constraints were explicit. The constraints were enforced explicitly at the midpoint and endpoint of each time step.

Numerical simulations using the various formulations of the dynamic system showed that accurate results, based on energy conservation and constraint violation, could be achieved using several of the formulations. The traditional approach of solving ordinary differential equations yielded good results, as expected, but calculations performed using the nonlinear algebraic equations associated with the direct solution with implicit constraints conserved energy better and would appear to be better suited for very long simulations. Somewhat surprisingly, solutions obtained from a direct solution for which the displacement constraint was enforced at the endpoint of each time step yielded results that were superior to results from the ordinary differential equations and the implicit direct solution.

Numerical solutions of the differential-algebraic equations produced adequate results in terms of the velocity and displacement constraints being enforced. However, the rms change in energy over the duration of the simulation was quite large, as compared with the simulations using the ordinary differential equations and the algebraic equations in which the constraints were enforced implicitly or explicitly at the end of each time step. This concern, in addition to the extra analytical effort required for the index reduction, would appear to render this solution method to be less desirable than the others for numerical simulations.

The direct solution in which the displacement constraint was enforced explicitly at the midpoint of each time step failed to yield an adequate solution. It was able to reduce the violation of the velocity constraints at the midpoint and the displacement constraints at the endpoint of each time step. However, it was not able to exert sufficient control over the velocity at the endpoint, which resulted in its inability to conserve the total energy of the system.

In conclusion, it has been shown that direct solutions based on Hamilton's law of varying action are capable of achieving numerical results that are equal or superior to numerical results obtained from ordinary differential equations or differential-algebraic equations. It is important to emphasize that when performing numerical simulations using direct methods in which the constraints are explicit the numerical accuracy and stability of the solution requires that the constraints be enforced at the end of each time step. Although direct methods may not be sufficient for every analysis requirement, they deserve to be considered as an excellent alternative for applications that focus on numerical simulations.

Acknowledgments

This work was supported by the U.S. Air Force Office of Scientific Research under Military Interdepartmental Purchase Request F1AT A07073G01. The Program Manager for this research is Victor Giurgiutiu.

References

[1] Bailey, C. D., "Application of Hamilton's Law of Varying Action," *AIAA Journal*, Vol. 13, No. 9, Sept. 1975, pp. 1154–1157.

doi:10.2514/3.6966
[2] Bailey, C. D., "Exact and Direct Analytical Solutions to Vibrating Systems with Discontinuities," *Journal of Sound and Vibration*, Vol. 44, No. 1, Jan. 1976, pp. 15–25. doi:10.1016/0022-460X(76)90703-3
[3] Bailey, C. D., "Direct Analytical Solutions to Non-Uniform Beam Problems," *Journal of Sound and Vibration*, Vol. 56, No. 4, April 1978, pp. 501–507. doi:10.1016/0022-460X(78)90292-4
[4] Bailey, C. D., "Hamilton's Law and the Stability of Nonconservative Continuous Systems," *AIAA Journal*, Vol. 18, No. 3, March 1980, pp. 347–349. doi:10.2514/3.7662
[5] Hodges, D. H., "Direct Solution for Sturm–Liouville Systems with Discontinuous Coefficients," *AIAA Journal*, Vol. 17, No. 8, Aug. 1979, pp. 924–926. doi:10.2514/3.61252
[6] Borri, M., Ghiringhelli, G., Lanz, M., Mantegazza, P., and Merlini, T., "Dynamic Response of Mechanical Systems by a Weak Hamiltonian Formulation," *Computers and Structures*, Vol. 20, No. 1, Jan. 1985, pp. 495–508. doi:10.1016/0045-7949(85)90098-7
[7] Borri, M., and Mantegazza, P., "Non Linear Oscillations and Limit Cycles: A Numerical Approach by Finite Elements in Time Domain," *Sixth International Conference on Mathematical Modelling*, Washington Univ. Inst. for Applied Sciences, Aug. 1987..
[8] Hodges, D. H., and Bless, R. R., "A Weak Hamiltonian Finite Element Method for Optimal Control Problems," *Journal of Guidance, Control, and Dynamics*, Vol. 14, No. 1, 1991, pp. 148–156. doi:10.2514/3.20616
[9] Kunz, D. L., "Multibody System Analysis Based on Hamilton's Weak Principle," *AIAA Journal*, Vol. 39, No. 12, Dec. 2001, pp. 2382–2388. doi:10.2514/2.1246
[10] Baruch, M., and Riff, R., "Hamilton's Principle, Hamilton's Law—6*n* Correct Formulations," *AIAA Journal*, Vol. 20, No. 5, May 1982, pp. 687–692. doi:10.2514/3.7937
[11] Riff, R., and Baruch, M., "Finite Element Discretization of Hamilton's Law of Varying Action," *AIAA Journal*, Vol. 22, No. 9, Sept. 1984, pp. 1310–1318. doi:10.2514/3.48566
[12] Riff, R., and Baruch, M., "Stability of Time Finite Elements," *AIAA Journal*, Vol. 22, No. 8, Aug. 1984, pp. 1171–1173. doi:10.2514/3.8755
[13] Hulbert, G. M., "Time Finite Elements for Structural Dynamics," *International Journal for Numerical Methods in Engineering*, Vol. 33, No. 2, 1992, pp. 307–331. doi:10.1002/nme.1620330206
[14] Chung, J., and Hulbert, G. M., "A Time Integration Algorithm for Structural Dynamics with Improved Numerical Dissipation: The Generalized-α Method," *Journal of Applied Mechanics*, Vol. 60, No. 2, June 1993, pp. 371–375. doi:10.1115/1.2900803
[15] Borri, M., Bottasso, C. L., and Trainelli, L., "Integration of Elastic Multibody Systems by Invariant Conserving/Dissipating Algorithms 1: Formulation," *Computer Methods in Applied Mechanics and Engineering*, Vol. 190, Nos. 29–30, 2001, pp. 3669–3699. doi:10.1016/S0045-7825(00)00286-3
[16] Bauchau, O. A., Bottasso, C. L., and Trainelli, L., "Robust Integration Schemes for Flexible Multibody Systems," *Computer Methods in Applied Mechanics and Engineering*, Vol. 192, Nos. 3–4, 2003, pp. 395–420. doi:10.1016/S0045-7825(02)00519-4
[17] Junkins, J. L., and Lee, S., "Validation of Finite-Dimensional Approximate Solutions for Dynamics of Distributed-Parameter Systems," *Journal of Guidance, Control, and Dynamics*, Vol. 18, No. 1, Jan. 1995, pp. 87–95. doi:10.2514/3.56661
[18] Brenan, K. E., Campbell, S. L., and Petzold, L. R., *Numerical Solution of Initial-Value Problems in Differential-Algebraic Equations*, Vol. 14, Classics in Applied Mathematics, Society for Industrial and Applied Mathematics, Philadelphia, 1996.
[19] Meirovitch, L., *Methods of Analytical Dynamics*, McGraw–Hill, New York, 1970.
[20] Hindmarsh, A. C., "LSODE and LSODI, Two New Initial Value Ordinary Differential Equation Solvers," *Signum Newsletter*, Vol. 15, No. 4, 1980, pp. 10–11. doi:10.1145/1218052.1218054
[21] Radhakrishnan, K., and Hindmarsh, A. C., "Description and Use of LSODE, the Livermore Solver for Ordinary Differential Equations," NASA, Ref. Publ. NASA-RP-1327, 1993.
[22] Powell, M. J. D., "A Hybrid Method for Nonlinear Equations," *Numerical Methods for Nonlinear Algebraic Equations*, Gordon and Breach, New York, 1970, pp. 87–114.
[23] Bauchau, O. A., "A Self-Stabilized Algorithm for Enforcing Constraints in Multibody Systems," *International Journal of Solids and Structures*, Vol. 40, Nos. 13–14, 2003, pp. 3253–3271. doi:10.1016/S0020-7683(03)00159-8

R. Kapania
Associate Editor